

# Post-mortem neuropathologic examination of a 6-case series of CAR T-cell treated patients

Nuria Vidal-Robau<sup>1\*</sup>, Gabriela Caballero<sup>1\*</sup>, Ivan Archilla<sup>1</sup>, Andrea Ladino<sup>2</sup>, Sara Fernández<sup>2</sup>, Valentín Ortiz-Maldonado<sup>3</sup>, Montserrat Rovira<sup>3</sup>, Marta Gómez-Hernando<sup>3</sup>, Julio Delgado<sup>3</sup>, María Suárez-Lledó<sup>3</sup>, Carlos Fernández de Larrea<sup>3,8</sup>, Olga Balagué<sup>1</sup>, Gerard Frigola<sup>1</sup>, Abel Muñoz<sup>1</sup>, Estrella Ortiz<sup>1</sup>, Teresa Ribalta<sup>1</sup>, Miguel J. Martínez<sup>5,6</sup>, Maria Angeles-Marcos<sup>5</sup>, Marta Español-Rego<sup>7</sup>, Azucena González<sup>7</sup>, Daniel Benitez-Ribas<sup>7</sup>, Eugenia Martinez-Hernandez<sup>4</sup>, Pedro Castro<sup>2,8</sup>, Iban Aldecoa<sup>1,9</sup>

<sup>1</sup> Pathology Department, Biomedical Diagnostic Centre (CDB), Hospital Clinic of Barcelona – University of Barcelona, Barcelona, Spain

<sup>2</sup> Medical Intensive Care Unit, Hospital Clinic of Barcelona – University of Barcelona, Barcelona, Spain

<sup>3</sup> Haematology Department, Hospital Clinic of Barcelona – University of Barcelona, Barcelona, Spain

<sup>4</sup> Neurology Department, Hospital Clinic of Barcelona – University of Barcelona, Barcelona, Spain

<sup>5</sup> Microbiology Department, Biomedical Diagnostic Centre (CDB), Hospital Clinic of Barcelona – University of Barcelona, Barcelona, Spain

<sup>6</sup> Barcelona Institute for Global Health (ISGlobal), Hospital Clinic of Barcelona – University of Barcelona, Barcelona, Spain

<sup>7</sup> Immunology Department, Biomedical Diagnostic Centre (CDB), Hospital Clinic of Barcelona – University of Barcelona, Barcelona, Spain

<sup>8</sup> August Pi Sunyer Biomedical Research Institute (IDIBAPS) – University of Barcelona, Barcelona, Spain

<sup>9</sup> Neurological Tissue Bank, Biobank of Hospital Clinic of Barcelona – IDIBAPS, Barcelona, Spain

\* These authors contributed equally

Corresponding author:

Iban Aldecoa Ansorregui · Pathology Department. 3<sup>rd</sup> stair, 5<sup>th</sup> floor · Hospital Clinic of Barcelona · St. Villarroel 170 · 08036 Barcelona · Spain

[ialdecoa@clinic.cat](mailto:ialdecoa@clinic.cat)

Submitted: 04 August 2022 · Accepted: 20 October 2022 · Copyedited by: Alessia Sciortino · Published: 27 October 2022

## Abstract

**Introduction:** Chimeric antigen receptor (CAR) T-cell therapy is a promising immunotherapy for the treatment of refractory hematopoietic malignancies. Adverse events are common, and neurotoxicity is one of the most important. However, the physiopathology is unknown and neuropathologic information is scarce.

**Materials and methods:** Post-mortem examination of 6 brains from patients that underwent CAR T-cell therapy from 2017 to 2022. In all cases, polymerase chain reaction (PCR) in paraffin blocks for the detection of CAR T cells was performed.

**Results:** Two patients died of hematologic progression, while the others died of cytokine release syndrome, lung infection, encephalomyelitis, and acute liver failure. Two out of 6 presented neurological symptoms, one with extracranial malignancy progression and the other with encephalomyelitis. The neuropathology of the latter showed severe perivascular and interstitial lymphocytic infiltration, predominantly CD8+, together with a diffuse interstitial histiocytic infiltration, affecting mainly the spinal cord, midbrain, and hippocampus, and a diffuse gliosis of basal ganglia, hippocampus, and brainstem. Microbiological studies were negative for neurotropic viruses, and PCR failed to detect CAR T-cells. Another case without detectable neurological signs showed cortical and subcortical gliosis due to acute hypoxic-ischemic damage. The remaining 4 cases only showed a mild patchy gliosis and microglial activation, and CAR T cells were detected by PCR only in one of them.

**Conclusions:** In this series of patients that died after CAR T-cell therapy, we predominantly found non-specific or minimal neuropathological changes. CAR T-cell related toxicity may not be the only cause of neurological symptoms, and the autopsy could detect additional pathological findings.

**Keywords:** Hematologic malignancies, Chimeric antigen receptor (CAR) T-cell, Cytokine release syndrome (CRS), Neurotoxicity, Neuropathology, Immunohistochemical stains

## Introduction

Chimeric antigen receptor (CAR) T-cell therapy is a promising immunotherapy for the treatment of refractory hematopoietic malignancies. Normal and malignant B-cells express the CD19 protein in the cell membrane. Lymphodepletion followed by transfer of autologous T-cells that have been genetically modified to express a CAR targeting CD19 have been effective in clinical trials, producing remission of refractory or relapsed acute lymphoblastic leukemia (ALL), chronic lymphocytic leukemia and non-Hodgkin's lymphoma (NHL)<sup>1-5</sup>. Recently, BCMA targeted CARs have been used to treat multiple myeloma<sup>6</sup>.

Among toxic effects expected after lymphodepletion and anti-CD19 CAR T-cell infusion, cytokine release syndrome (CRS) and neurotoxicity are the most relevant but, unlike CRS, the physiopathology of neurological events is less known and neuropathologic information is scarce<sup>7</sup>. Clinical presentation develops mostly as non-specific brain dysfunction without focal signs, most of them being mild and

transient. Nevertheless, focal symptoms such as seizures and fatal cerebral oedema have been described.

Neurotoxicity can occur in the context of severe CRS, where disruption of the blood-brain barrier (BBB) by cytokine production and subsequent endothelial activation leads to an increase in proinflammatory cytokine levels in cerebrospinal fluid (CSF)<sup>7-10</sup>. However, neurotoxicity is also associated with expansion and activation of CAR T-cells that lead to a direct parenchymal CAR T-cell infiltration. In addition to CRS following CAR T-cell infusion, factors that favor CAR T-cell proliferation in blood, such as the addition of fludarabine to cyclophosphamide lymphodepletion chemotherapy<sup>9</sup>, are also associated with an increased risk of neurotoxicity. Fludarabine is an antineoplastic agent that added to the conditioning regimens improves the expansion and persistence of CAR T-cells, as well as duration of remission and disease-free survival<sup>2,4,5</sup>. Its contribution to neurotoxicity may be driven by different mechanisms, and is yet to be elucidated. However,

fludarabine-associated neurotoxicity has a later onset, and cerebral oedema is not usually reported<sup>11</sup>.

Reports of neuropathological findings after CAR T-cell therapy are scarce, independent of the presence or absence of neurological symptoms prior to death. We only found 4 cases described in the literature, which showed variable and non-specific neuropathological changes<sup>7–10</sup>. Here, we report detailed neuropathological findings of 6 patients who died after CAR T-cell therapy<sup>12</sup>.

## Materials and methods

Six brains from patients that underwent CAR T-cell therapy from 2017 to 2022 in a tertiary university hospital were examined. We selected all cases with CAR T-cell therapy from requested medical autopsies at the Pathology Department during this period. Patients received ARI-0001 (anti-CD19) and ARI-0002h (anti-BCMA, for patients with multiple myeloma) based CAR T treatment. For ARI-0001, the planned target cell dose varied depending on the patient's disease: typically,  $1 \times 10^6$  ARI-0001 cells/kg for patients with acute lymphoblastic leukemia and chronic lymphocytic leukemia; and  $5 \times 10^6$  ARI-0001 cells/kg for non-Hodgkin lymphoma patients. Full details of ARI-0001 and ARI-0002h cell production and a phenotypic characterization of these cells can be found elsewhere<sup>6,12–14</sup>. Clinical data was retrospectively retrieved from the electronic medical records. Formalin-fixed and paraffin-embedded tissue sections from the frontal cortex, visual cortex, cingulate, hippocampus, amygdala, thalamus, basal ganglia, white matter, midbrain, pons, medulla oblongata, spinal cord and cerebellum that had been stained with hematoxylin-eosin (HE) were histologically assessed using light microscopy. In some of the cases the study was extended with immunohistochemistry (IHC). IHC was performed on 5- $\mu$ m formalin-fixed, paraffin-embedded (FFPE) sections using the Roche Benchmark Ultra platform with usual antigen retrieval protocols. The primary antibodies used were CD3 (2GV6, Roche), CD20 (L26, Roche), CD4 (SP35, Roche), CD68 (KP-1, Roche), Glial fibrillary acidic protein (GFAP) (EP672Y, Roche), Terminal deoxynucleotidyl transferase (TdT) (Roche), Beta amyloid (DE2B4, Roche), TAU (AT8, Thermo-Fisher

Scientific), Neurofilament (2F11, Roche), Herpes simplex virus (HSV)-1 (10A3, Roche), HSV2 (DBM15.69, Sanbio), Human herpes virus (HHV)-6 (A & B, gp 60/110, Millipore), HHV-8 (13B10, Roche), Cytomegalovirus (CMV) (8B1.2, 1G5.2, and 2D4.2, Roche), Epstein-Barr virus (EBV) latent membrane protein (LMP)-1 (CS1-4, Roche), Epstein-Barr virus (EBV)-encoded small RNAs (EBER) (Roche), and Pol-yomavirus (MRQ-4, Roche). IHC studies were performed in the initial diagnostic workup when clinical suspicion or neuropathological evidence of any pathologic process was observed. In addition, a systematic retrospective analysis was performed: CD3 and CD20 were screened on hippocampal and mid-brain sections in all cases, on spinal cord sections in all cases except case 1, on frontal cortex in all cases except cases 2 and 3, and on basal ganglia only in cases 4 and 6. GFAP IHC was performed on frontal sections in all cases, on basal ganglia in all cases except case 3, on hippocampus in all cases except case 1, and on midbrain only in case 4.

Polymerase chain reaction (PCR) in paraffin blocks was performed in case 5 for the detection of HHV-6, West Nile virus, adenovirus, enterovirus, measles, mumps and lymphocytic choriomeningitis. Samples of all cases from hippocampus, midbrain, and spinal cord (only in cases 2 to 6) were used for CAR T-cell detection by PCR. Five micrometer sections were obtained from paraffin blocks, and DNA was extracted using QIA amp DNA FFPE Tissue Kit (QIAGEN, Hilden, Germany). Real-time PCR was used to measure number of copies/cell. Genomic DNA was amplified as previously described<sup>13</sup>. Amplification reactions were performed in triplicate. An eight-point standard curve was generated using a sequence close to the CDKN1A gene (GENEBANK: Z86995) as comparator. The test was calibrated to detect a number of copies ranging from 5 to 106 per 500 ng of genomic DNA.

## Results

See Table 1 for a summary of the cases here presented and the other cases reported in the literature, and Figure 1 for the comparison of gliosis and T-cell infiltrates of the cases.

**Table 1.** Clinical data and histopathologic findings of our cases and previously described cases (modified from<sup>7</sup>)

No. of patient/ Ref.	Age, gender (M – F)	Disease	Product	Cy/flu conditioning	Corticoids in last admission	Cause of Death	Time between CAR-T infusion and death	Neurologic signs	Autopsy findings	CAR T-cells in FFPE brain tissue
1	44, F	B-cell lymphoblastic leukemia	ARI-0001 (CAR T 19)	Yes	Yes	Disease progression and signs of pneumonia and pulmonary hemorrhage	23 days	Yes	Mild changes and occasional intravascular leukemia cells: Mild arteriosclerosis and arteriolar hyalinosis, minimal T-cell perivascular infiltrate, occasional intravascular infiltration by TdT positive atypical cells (leukemic cells), without remarkable parenchymal involvement.	Negative
2	19, F	Mediastinal diffuse large B-cell lymphoma	ARI-0001 (CAR T 19)	Yes	Yes	Disease progression and signs of pneumonia.	33 days	No	Mild changes: mild gliosis in basal ganglia and occasional perivascular hemosiderin deposits in parenchymal blood vessels of the white matter and basal ganglia.	Positive
3	19, M	B-cell acute lymphoblastic leukemia	ARI-0001 (CAR T 19)	Yes	Yes	Cytokine release syndrome	5 days	No	Mild changes: Mild white matter oedema with mild gliosis in basal ganglia and midbrain tegmentum. Cortical dark neurons suggestive of incipient hypoxic-ischemic alterations. Mild congestion and minimal arteriosclerosis of parenchymal blood vessels with occasional perivascular histiocytes.	Negative
4	63, M	Follicular lymphoma	ARI-0001 (CAR T 19)	Yes	Yes	Respiratory failure due to nosocomial pneumonia	5 months	No	Cortical gliosis in frontal and parahippocampal cortices, in possible relation to mild acute hypoxic-ischemic injury, with scattered foci of gliosis with minimal clasmotodendrosis in frontal and parahippocampal subcortical white matter. Mild arteriosclerosis and arteriolar hyalinosis.	Negative
5	28, M	B-cell acute lymphoblastic leukemia	ARI-0001 (CAR T 19)	Yes	Yes	Encephalomyelitis	43 days	Yes	Diffuse lymphocytic encephalomyelitis: Diffuse gliosis in basal ganglia, hippocampus, brainstem, and spinal cord. Severe interstitial and perivascular lymphocytic (CD3+ and predominantly CD8+) and histiocytic infiltrates in anterior horns and grey matter of spinal cord, as well as brainstem, limbic system, and basal ganglia. Mild focal clasmotodendrosis in hippocampal white matter.	Negative

6	71, F	Multiple Myeloma	ARI-0002 (CAR T BCMA)	Yes	Yes	Submassive liver necrosis of probable ischemic cause	19 days	No	Mild changes: Minimal diffuse gliosis and minimal microglial activation. Isolated perivascular T-cells. Mild arteriosclerosis.	Negative
Torre et al., 2018	21, M	B-ALL	JCAR015	Yes	Yes	Fulminant cerebral edema	4 days	Yes	Expansion of perivascular spaces attributed to blood-brain barrier dysfunction, clasmotodendrosis with perivascular distribution of damaged astrocytes within white matter, myelin pallor and vacuoles within white matter, few scattered intraparenchymal inflammatory cells and rare T-cells; perivascular macrophages clusters, microglia activation.	Negative
Gust et al., 2017	N/A	B-cell malignancy	CD19 CAR	N/A	N/A	Brainstem hemorrhage	13 days	N/A	Evidence of CAR T-cells in perivascular areas and CSF, with evidence of blood and blood-brain barrier alterations, with Intravascular vWF binding and CD61-positive platelet microthrombi, and parenchymal lesions with multifocal microhemorrhages, patchy parenchymal necrosis and fibrinoid vessel wall necrosis. Reactive microglia without diffuse activation.	Positive
Gust et al., 2017	N/A	B-cell malignancy	CD19 CAR	N/A	N/A	Severe CRS, multiorgan failure, grade 4 neurotoxicity	N/A	N/A	Intravascular CD61-positive platelet microthrombi.	N/A
Schuster et al., 2017	N/A	Follicular lymphoma	CTL019 (CD19/4-1BB)	Yes	No	Progressive neurologic deterioration	N/A	Yes	Inflammatory process with dense macrophage infiltration of white matter, microglial activation and a moderate CD8+ T-cell infiltrate with white matter degeneration, gliosis, and neuronal loss. No evidence of herpes simplex virus 1 or 2, cytomegalovirus, varicella-zoster virus, JC virus, adenovirus, or Epstein-Barr virus	N/A

M: male; F: female; N/A: not applicable. FFPE: Formalin fixed paraffin embedded.

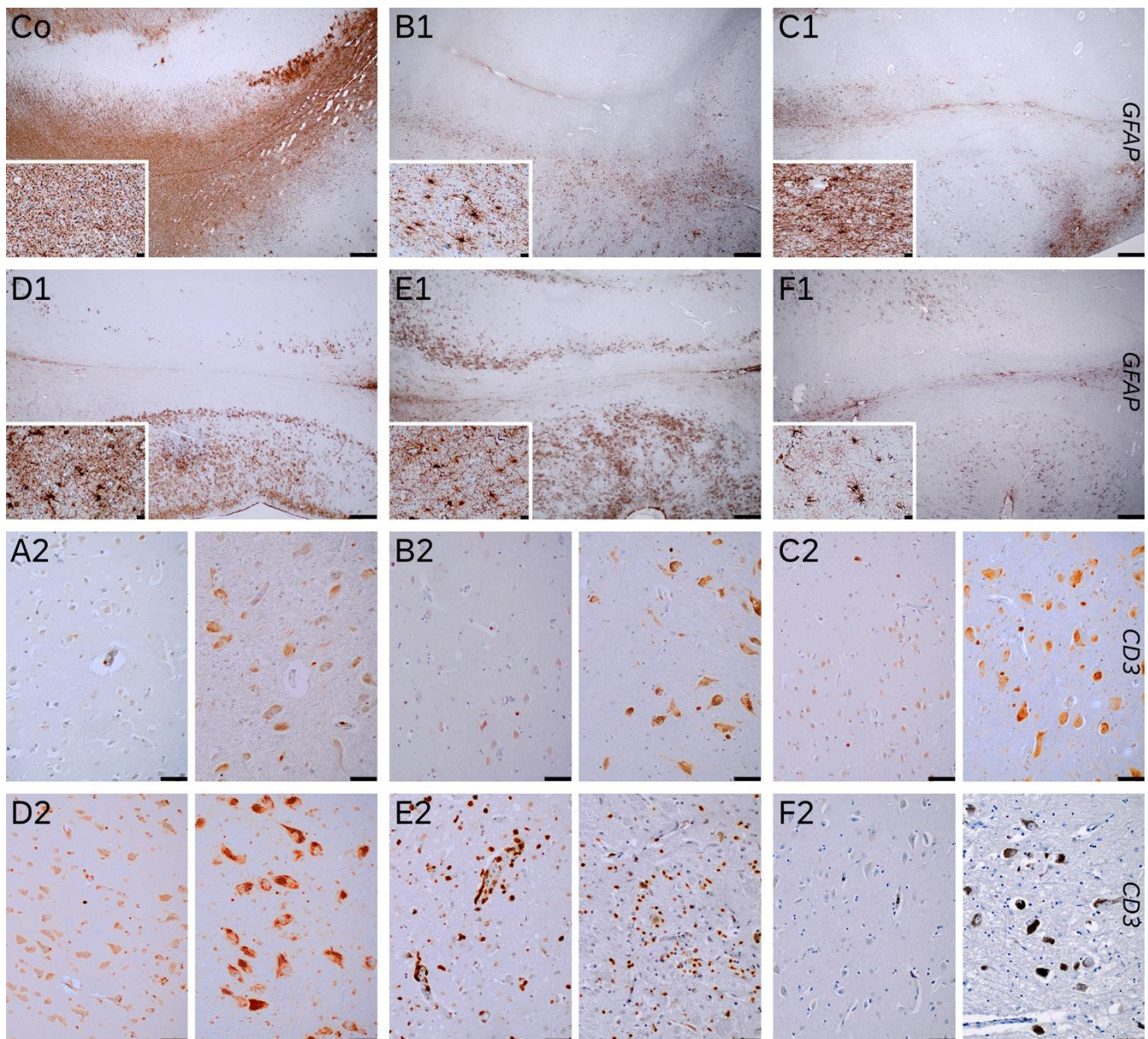


**Figure 1.** Figures Co to F1: GFAP immunohistochemistry of hippocampus (upper third CA1 sector -right side- and subiculum – left side-) and parahippocampal area (lower third, transentorhinal cortex) of a control (Co) and cases 2 (B1), 3 (C1), 4 (D1), 5 (E1) and 6 (F1). The control was a 52-year-old male who died due to an acute bilateral adrenal hemorrhage with extensive clasmotodendrosis (insets, parahippocampal white matter, 400x). The cases showed variable gliosis, predominantly mild, higher in case 5 (E1) who had an encephalitis, and case 4 (D1) who died with an extensive acute pneumonia. Both had mild and isolated clasmotodendritic changes in white matter (see insets).

Row 3 and 4 show T-cell infiltrates (CD3+) in parahippocampal cortex (left half) and substantia nigra pars compacta (right half), in cases 1 (A2), 2 (B2), 3 (C2), 4 (D2), 5 (E2) and 6 (F2). Only case 5 (E2) presented marked infiltrates, while other cases has only scattered to isolated perivascular T-cells. Case 2 (B2), which was positive for CART PCR in brain tissue, did not have significantly higher T-cell infiltrates (Figures Co, B1 to F1 20x scale bar 500 µm; insets 400x, scale bar 20 µm). Figures A2 to F2 200x, scale bar 50 µm).

## Case 1

A 44-year-old woman with acute B-cell lymphoblastic leukemia presented to an outside hospital with central nervous system (CNS) involvement and a paravertebral mass (D8-D10) without spinal compression. At disease onset, she had lymph node involvement and leukocytosis and was refractory to five lines of treatment. At her first consultation in our center she did not present any neurological symptoms. Basal brain Magnetic Resonance Imaging (MRI) showed a nonspecific lacunar lesion in the left frontal white matter and discrete homogeneous dural enhancement in cerebral convexity; the cerebrospinal fluid (CSF) study was normal. After the conditioning with cyclophosphamide and fludarabine, she received CAR-CD19 treatment. Three days after the infusion she developed fever, pulmonary interstitial infiltrates, and pleural effusion. The radiology was suggestive of non-cardiogenic oedema, with isolated colonies of *Staphylococcus haemolyticus* in respiratory samples culture. She received antimicrobial therapy, depletive treatment, pleural drainage, and non-invasive mechanical ventilation, as well as tocilizumab, as a CRS could not be ruled out. Her clinical status improved, although she had persistent fever with negative microbiological culture. Fourteen days after the infusion she progressed with fever, hemodynamic instability and multi organ failure, as well as CAR T-cells amplification in peripheral blood. With the diagnosis of CRS, a second dose of tocilizumab was administered with only partial improvement. Steroids were added, but the patient developed confusion, suggesting neurotoxicity. The electroencephalogram (EEG) showed generalized slowing, compatible with encephalopathy, and the brain MRI showed two non-specific signal abnormalities/foci of signal alteration without mass effect or contrast uptake, lateral to the left ventricular atrium and in the right temporo-occipital area adjacent to the ventricular occipital horn. Flow cytometry (FC) of the CSF revealed the presence of mature T lymphocytes and isolated blasts, and the microbiological CSF study was weakly positive for HHV-6. Nineteen days after the infusion she presented rapidly progressive respiratory and hemodynamic deterioration requiring intubation and vasoactive treatment. The tracheal aspirate was positive for *Stenotrophomonas maltophilia* and the diagnostic of septic shock

due to nosocomial pneumonia was established. Antibiotic treatment was escalated. However, she progressed with pulmonary hemorrhage and died 23 days after the infusion.

Neuropathologic gross examination revealed a 1280 g fixed brain with diffuse petechiae in the dura mater. Coronal sections showed slight discoloration of right temporal white matter. Histology showed mild arteriosclerosis and arteriolar hyalinosis, minimal lymphocytic perivascular infiltrate (T-cell predominant) and occasional intravascular infiltration by atypical cells with TdT positivity (Figure 2), confirming the presence of leukemic cells, without remarkable parenchymal involvement. CAR T-cell PCR in the brain was negative and there were no signs suggestive of encephalitis associated to viral infection.

Full body autopsy demonstrated massive dissemination of the lymphoproliferative process affecting the lungs, liver, spleen, bone marrow, lymph nodes and mammary gland. The cause of death was attributed to disease progression.

## Case 2

A 19-year-old woman presented with primary mediastinal diffuse large B-cell lymphoma with infiltration of soft tissues. She had a protracted course with persistent mediastinal disease, gastric relapse, superior vena cava syndrome and pericardial and pleural malignant effusions. She received multiple therapy lines including autologous stem cell transplant, local radiotherapy, and several chemotherapy lines comprising burkimab protocol and ibrutinib, before considering CAR T treatment. Her initial MRI showed mild global cerebral atrophy without other remarkable findings. On admission she was hypotensive and tachycardic and Positron Emission Tomography (PET) – Computed Tomography (CT) scan showed pericardial infiltration in addition to supra and infradiaphragmatic lymphadenopathies, with soft tissue, muscle, bone, and pleural multifocal enhancement. The presence of bone marrow aplasia delayed the conditioning with fludarabine-cyclophosphamide. Respiratory distress increased after conditioning along with the pleural effusion, and she was admitted to the intensive care unit (ICU) to receive CAR-CD19 infusions. The following 48 hours,

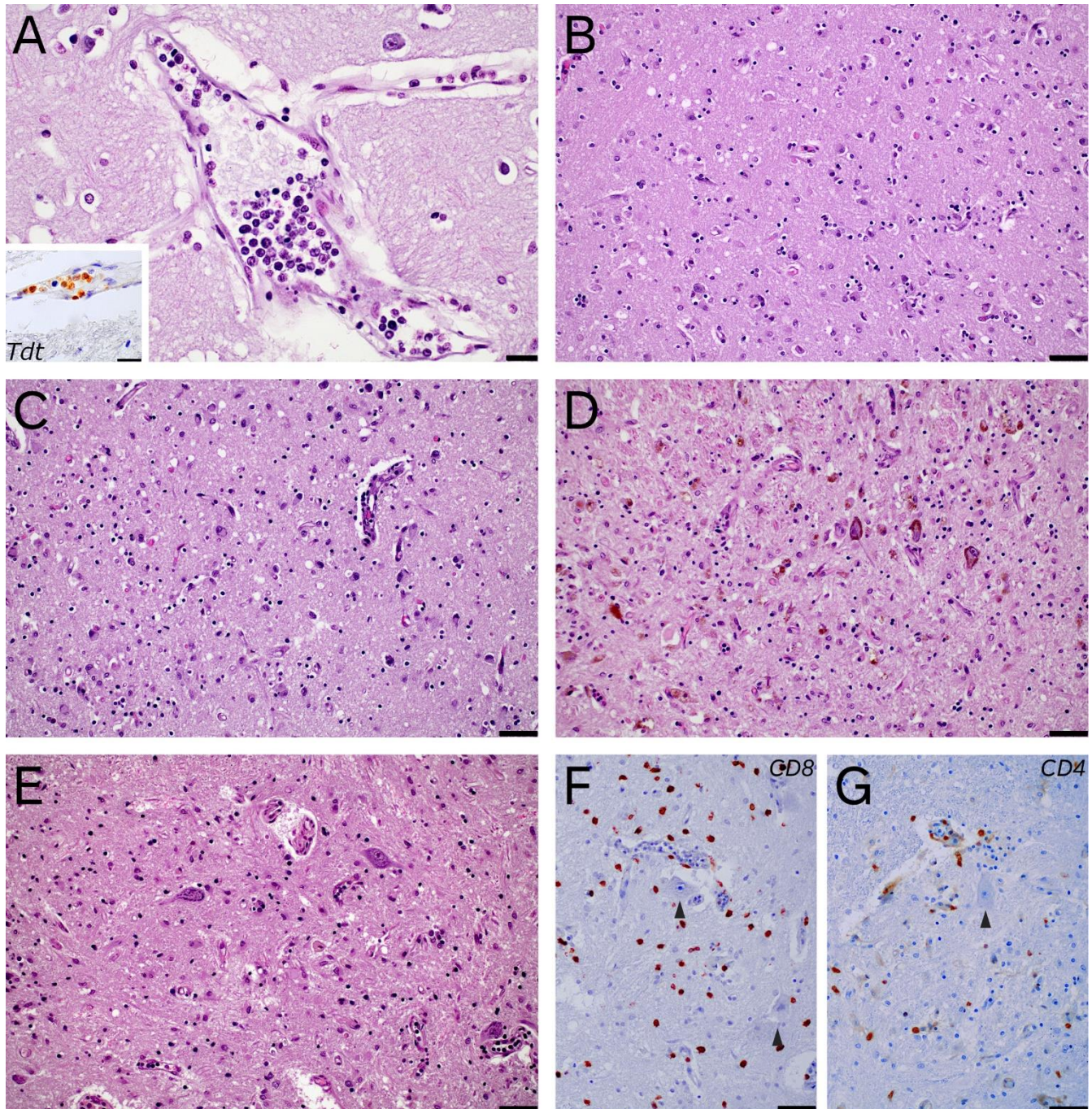


**Figure 2.** Remarkable histological features: case 1 presented scant intravascular infiltration of the leukemia (A), which was positive for Tdt (A, inset). Case 5 showed an encephalomyelitis, with predominant involvement of limbic areas (B, entorhinal cortex), basal ganglia (C, hypothalamus), brainstem (D, substantia nigra) and spinal cord (E, lumbar spinal cord). T-cell lymphocytic infiltrates were both CD8+ and CD4+, with predominance of the former (F and G, CD8+ and CD4+ infiltrates in lumbar spinal cord, which did not show marked tropism for motor neurons (arrowheads)) (A 400x, scale bar 20  $\mu$ m, inset 600x, scale bar 20  $\mu$ m; B to G, 200x, scale bar 50  $\mu$ m).

her respiratory status worsened, adding hemodynamic instability and fever. A nosocomial pneumonia was diagnosed by X-ray and ultrasound examination, without microbiological isolation, and she received antibiotics and fluconazole. Despite treatment, her status worsened, requiring invasive me-

chanical ventilation and vasoactive treatment. Subsequently, she presented superior vena cava syndrome and worsening of pericardial effusion with progression of hemodynamic instability. Although she received corticosteroids and rituximab aiming to diminish the tumoral mass, she progressed to or-

ganic failure, and died 33 days after CAR T infusion. Neurological symptoms were not detected in the course of the disease, although it was difficult to examine the patient due to sedation administered during invasive mechanical ventilation. Neuropathologic gross examination was unavailable. Histology revealed basal ganglia mild gliosis, and occasional perivascular hemosiderin deposits in parenchymal blood vessels of the white matter and basal ganglia. Immunohistochemical studies showed scarce perivascular CD3+ T-cells with minimal intraparenchymal extension in the midbrain tegmentum, as well as in perithalamic white matter and cervical spinal cord. T-cells were not detected in the hippocampus, and there were almost no CD20+ B-cells. PCR for the detection of CAR T-cells in paraffin blocks of midbrain and spinal cord was positive, while it was negative in the hippocampus.

Full body autopsy revealed a large mediastinal mass with pericardial extension causing severe constrictive pericarditis, as well as extension to cervical region, diaphragm, rib wall and skin, and multiorgan tumor implants. No clear histological signs of acute neutrophilic pneumonia were found, although the immunosuppressive and neutropenic status may have had hindered the presence of histological signs. The cause of death was attributed to disease progression.

### Case 3

A 19-year-old man with acute B-cell lymphoblastic leukemia was referred to our center one year after disease onset. He had relapsed disease despite induction protocol and six consolidation treatment cycles, as well as one cycle of inotuzumab-ozogamicine. He received cyclophosphamide and corticosteroid bolus as bridge therapy before the infusion of CAR-CD19. His initial brain MRI showed multiple bilateral cortical and subcortical frontoparietal signal abnormalities suggesting chronic hemorrhages from multiple cerebral cavernomatosis, but no contraindication for the CAR T therapy was found. After conditioning with fludarabine and cyclophosphamide, antibiotics were started due to fever and isolation of *Enterococcus faecalis* in urine culture. Twelve hours after the first CAR T-cell infusion, he presented fever and hemodynamic instability re-

fractory to fluids. He was transferred to the intensive care unit (ICU) with the diagnosis of CRS grade 3. Tocilizumab, high doses of methylprednisolone and siltuximab, as well as support treatment with several vasopressors, mechanical ventilation, and empirical treatment with antifungal and antibacterial agents were administered. However, he developed refractory multiorgan failure, with negative microbiological analyses, and he died five days after CAR T-cell infusion. No neurological symptoms were noted, and he was clinically diagnosed as fatal CRS (grade 5).

Neuropathologic gross examination revealed a 1255 g fixed brain. Coronal sections showed mild congestive appearance of left amygdala, putamen, front-temporo-parieto-occipital white matter, and pontine nuclei, as well as mild greyish discoloration of white matter, midbrain tegmentum and pons. The brainstem showed moderate substantia nigra depigmentation.

Histology confirmed mild white matter oedema with mild gliosis, mainly in basal ganglia (ventral thalamus) and midbrain tegmentum/periaqueductal grey matter. Blue dark neurons were observed in cortical areas, predominantly in layers II and III, suggestive of incipient mild hypoxic-ischemic changes. Histology also revealed mild congestion and minimal arteriosclerosis of parenchymal blood vessels with occasional perivascular histiocytes with hematic component, without perivascular tissue damage. No evidence of venous dilations or vascular malformations were observed; the changes reported by MRI study were attributed to hemodynamic fluctuations in life rather than to the presence of established vascular malformations. PCR for the detection of CAR T-cells in paraffin blocks was negative.

Full body autopsy revealed no significant findings. The cause of death was attributed to CRS after CAR T-cell infusion.

### Case 4

A 63-year-old male patient with a grade 3A, stage IV follicular lymphoma with abdominal extranodal and mesenteric involvement that had been treated with a first line of R-CHOP and had reached

partial response. Following maintenance with rituximab for 2 years, he remained stable one more year, until progression of the abdominal mass, new gastric infiltration, and PET hypermetabolism in the esophagus. After a third line with obinotuzumab and bendamustine, a failed attempt of autologous stem cell aphaeresis, and maintenance with obinotuzumab, a fourth line with idelalisib was started. However, the abdominal disease progressed with involvement of peripancreatic, renal and iliac lymph nodes, the patient was not eligible to allogeneic stem cell transplant, and he received CAR-CD19 therapy with prior fludarabine and cyclophosphamide conditioning.

After the third day of consecutive infusion, the patient developed fever with mild hypotension that was diagnosed as grade 2 CRS and had a good response to tocilizumab. He had an episode of toxic epidermolytic necrolysis (diagnosed by skin biopsy) with severe extensive rash and oral lesions. He also presented with severe aplasia, as well as a septic shock due to urinary tract infection that was treated in the ICU. After initial improvement, he presented a pulmonary hemorrhage with colonization by *Candida glabrata*, and developed kidney failure, hyperkalemia, tracheobronchitis, more episodes of septic shock due to bacteremia of intestinal and skin origin (*Bacteroides fragilis*, *Pseudomonas aeruginosa*, *Enterococcus faecium*), and persistent candidemia as well as CMV reactivation. Due to persistent skin lesions, an alternative diagnosis of CAR T-cell associated dermatosis was suspected. Immunosuppression was restarted, improving the skin lesions, but it had to be stopped due to bone marrow aplasia and worsening neutropenia. Of note, the refractory follicular lymphoma showed morpho-metabolic decrease in post CAR T infusion CT and PET scans, attributed to the presence of circulating CAR T-cells. Eventually, the last episode of septic shock and ventilator associated pneumonia were refractory, which led to death after 4 months in the ICU at 5 months of CAR T-cell therapy. He died without evidence of neurological symptoms in the course of the disease, and a brain computerized tomography (CT) done 45 days after the CAR T infusions showed no significant findings.

Neuropathologic gross examination showed a 1240 g fixed brain. Coronal sections showed mild

congestive changes in caudate, putamen, thalamus, and parieto-occipital white matter.

Histology revealed cortical gliosis in frontal and parahippocampal cortices, in possible relation to acute hypoxic-ischemic injury, as well as mild scattered foci of gliosis with minimal clasmatodendrosis in frontal and parahippocampal subcortical white matter, highlighted with GFAP immunohistochemistry (see Figure 1). Mild parenchymal blood vessel arteriosclerosis and arteriolar hyalinosis, with occasional hemosiderin deposits, and isolated perivascular rarefaction in deep vessels was observed. Histology also showed isolated diffuse cortical amyloid beta deposits, and minimal amygdala neurofibrillary pathology. PCR for the detection of CAR T-cells in paraffin blocks was negative.

Full body autopsy excluded residual neoplasia and evidenced a pneumonic process in context of the septic condition. The final cause of death was a respiratory failure.

### Case 5

A 28-year-old man with B-cell acute lymphoblastic leukemia with disease progression with orbital infiltration. After diagnosis, induction, and consolidation treatment, he received haploidentical stem cell transplant (SCT), which was previously conditioned with thiotepa, fludarabine, busulfan and prophylaxis of graft versus host disease (GVHD) with tacrolimus and cyclophosphamide. He developed hemorrhagic cystitis, CMV reactivation, *Escherichia coli* orchitis and tacrolimus nephrotoxicity as complications, but never GVHD. He relapsed one year after SCT with testicular infiltration, which required blinatumomab rescue treatment and lymphocyte donor infusion plus intrathecal prophylaxis, but ultimately led to radiotherapy and posterior bilateral orchiectomy. Two years after diagnosis, he had progressive disease and was planned for CAR-CD19 therapy. His initial brain MRI showed few nonspecific subcortical white matter hyperintense signal abnormalities, and tumor infiltration of the right orbit. After lymphodepletion with fludarabine and cyclophosphamide, he received a first CAR T-cell infusion with good tolerance, no signs of CRS and good response observing non-neoplastic B-cells. Due to loss of CAR T-cells in peripheral blood, he received two reinfu-

sions in a 10-month period. The second was followed by an early loss of CAR T-cells due to antibodies, and the third infusion was made after plasma exchange to remove the antibodies. After the third infusion, he presented with fever without a clear origin that was treated with antibiotics, with low clinical suspicion of CRS due to the absence of analytical alterations. Almost one month after this last infusion, he presented with confusion, bradypsychia and generalized tremor. Repeated, a brain MRI showed no significant changes, and persistent tumor infiltration of the right orbit. EEG study showed diffuse slowing, and there were not significant findings in the CSF study. The neurological symptoms were refractory, and he died 43 days after the third CAR T-cell infusion.

Neuropathologic gross examination showed a 1385 g fixed brain. Coronal sections showed softening in both putamen.

Histology revealed diffuse gliosis predominant in basal ganglia, hippocampus, substantia nigra and brainstem. The most relevant finding was interstitial and perivascular lymphocytic infiltrates, together with histiocytic infiltrates, which were severe in anterior horns and grey matter of spinal cord, and to a lesser extent in the midbrain and hippocampus (Figure 2). Immunohistochemical studies revealed that lymphocytic infiltrates were CD3+ T-cells, predominantly CD8+, with practically no B-cells being observed, and were accompanied by severe CD68+ microglial activation with foamy histiocytes. Neurofilament staining showed occasional phosphorylated somas as well as isolated axonal spheroids in cortical and hippocampal white matter, without axonal loss in spinal cord tracts. GFAP staining showed mild and focal clasmatodendritic changes in the white matter. All the findings above were concordant with the diagnosis of a diffuse lymphocytic encephalomyelitis predominant in brainstem, spinal cord and limbic system, with milder disease in cortex and basal ganglia, and relative sparing of cerebellum. No viral inclusions were observed, and virus detection stains for HSV-1, HSV-2, HHV-6, HHV-8, CMV, EBV and polyomavirus, and PCR for HHV-6, West Nile virus, adenovirus, enterovirus, measles, mumps and lymphocytic choriomeningitis were negative. PCR in paraffin blocks for the detection of CAR T-cells was negative.

Full body autopsy revealed extensive pulmonary hemorrhage with no apparent signs of infection and foci of extramedullary hematopoiesis in the liver. After all, the cause of death was attributed to an unspecified encephalomyelitis, suggesting primarily an infectious etiology but not ruling out immune causes.

### Case 6

A 71-year-old woman with multiple myeloma IgA kappa R-ISS II, diagnosed from a scalp extramedullary plasmacytoma. Cytogenetic showed high risk (17p deletion) and it relapsed after four therapy lines. She received fludarabine and cyclophosphamide conditioning after bridging therapy. After one week of the first CAR-BCMA infusion, she was admitted to the ICU due to a grade 2 CRS with fever and hypotension that were successfully treated with one dose of tocilizumab and corticosteroids. Ten days later, she presented episodes of hypotension without fever or alterations in chest and brain CT or echocardiography. In the differential diagnosis, neurotoxicity related to treatment was considered, corticosteroid dose was increased, and antibiotics were added. She worsened with agitation, tachypnoea, and respiratory failure; and progressed to refractory multiorgan failure with ischemic hepatitis, renal failure, and hemorrhagic complications in the context of thrombocytopenia. A macrophagic activation syndrome was suspected due to LDH and ferritin increase, and treatment was attempted with corticosteroids, anakinra, siltuximab and cyclophosphamide. Amid this situation, she presented a blood culture positive for *Escherichia coli* without detectable septic focus. Despite all measures, she remained in multiorgan failure with acidosis and hyperlactacidemia, and she died 19 days after CAR T-cell therapy start. Additional neurotoxicity signs were not evident.

Neuropathologic gross examination showed a 1045 g fixed brain with mild hippocampal and amygdalar atrophy. Neuropathologic evaluation revealed mild arteriosclerosis (with focal mural calcification in globus pallidus arteries) and diffuse minimal gliosis. Histology revealed scattered perivascular T-cells (CD3+) in basal nuclei, frontal cortex, and hippocampus. Minimal microglial activation highlighted with CD68 accompanied these findings. She also had a

definite primary age related tauopathy or PART (Braak stage I/VI, Thal 0) and mild periamygdaline age related tau astrogliopathy or ARTAG. PCR for the detection of CAR T-cells in paraffin blocks was negative.

The most remarkable systemic finding was a submassive acute hepatic necrosis. The prominent center lobular location, the lack of cytopathic changes and negative immunohistochemical stains for HSV-1, HSV-2, HHV-8, CMV, EBV LMP1 and EBER oriented to a hemodynamic–hypovolemic etiology. There were additional acute hemorrhagic foci, like in myocardium and intestines, but the lack of tissue ischemia or inflammatory reaction surrounding them suggested they were acute premortem ischemic changes. Remarkably, there was hypercellular bone marrow with T-cell expansion and hemophagocytosis. Immunohistochemistry for CD68 in different organs showed moderate histiocytic activation in the spleen and mild activation in the heart, liver, intestine and brain. In the latter, it did not seem to induce secondary tissue alterations, hence its impact may have been limited. A lithic focus in the cranium was constituted mainly by fibrotic reactive tissue without evidence of plasma cell disease. After all, the cause of death was attributed to submassive liver necrosis of probable ischemic cause.

## Discussion

Here we present the neuropathological findings of 6 deceased patients, 3 women and 3 men, who received a CD19- (5) and BCMA- (1) targeted CAR T-cell therapy. Three of them had a B-cell acute lymphoblastic leukemia, one a follicular lymphoma 3A grade, one a primary mediastinal diffuse large B-cell lymphoma, and the other a multiple myeloma with plasmocytoma. Only 2 of them presented explicit neurological symptoms in the course of the disease.

Brain gross examination did not show significant alterations in any of the patients. Histological findings in one of the patients with neurological symptoms were mild arteriosclerosis and arteriolar hyalinosis, minimal lymphocytic perivascular infiltrate (mainly CD5+) and leukemic cells, in line with the systemic progression of the hematologic malignancy as the cause of death.

The histological examination of the other patient with neurological symptoms showed a severe perivascular and interstitial lymphocytic infiltration, predominantly CD8+, admixed with a diffuse interstitial histiocytic infiltration, affecting mainly the spinal cord, midbrain, and hippocampus, along with a diffuse gliosis of basal ganglia, hippocampus, and brainstem. Microbiologic studies were negative for neurotropic viruses, and PCR failed to detect CAR T-cells. Finally, the cause of death was attributed to a lymphocytic encephalomyelitis of unknown etiology, infectious versus toxic, without being able to demonstrate viral infection nor CAR T-cells in brain tissue. One of the cases without neurological signs showed mild clasmotodendrosis in context of terminal hypoxic-ischemic damage. The rest showed a mild patchy gliosis and microglial activation, with no other remarkable histologic changes. CAR T-cells were detected by PCR only in one of them, without histological particularities.

Reports of neuropathological findings after CAR T-cell therapy are scarce. Neuropathological findings in autopsies of different types of patients vary, but there are common changes suggesting astrocyte dysfunction, blood-brain barrier disruption with endothelial damage and activation, and a subsequent increase in vascular permeability. We found four cases described in the literature, all of them with neurological involvement that led to death. The autopsy of a patient who died from fulminant cerebral oedema showed signs of blood-brain-barrier disruption, clasmotodendrosis and microglial activation<sup>8</sup>. The findings in the autopsy of another patient who died from progressive neurologic deterioration were diffuse gliosis with severe neuronal loss and degeneration of white matter, dense infiltration of macrophages with numerous microglial cells, as well as a CD8+ infiltrate. It is worth noting that before the hematologic malignancy, he had the diagnosis of optic atrophy, which could alter the findings<sup>10</sup>. The autopsy findings of another 2 patients were vascular in nature, with multifocal microhemorrhages, perivascular infiltration of CD8+ cells, intravascular von Willebrand factor (vWF) binding, and platelet microthrombi, along with more severe vascular findings, such as karyorrhexis and fibrinoid vessel wall necro-

sis. Reactive microglia was also noted, the percentage of T-cells in the parenchyma mirrored the percentage of those cells in the CSF<sup>9</sup>.

It is worth highlighting that the clinical setting of patients undergoing CAR T-cell therapy makes it difficult to determine the cause of the observed neurological symptoms. While CRS is widely studied, neurological toxicity itself remains less understood. Neurological damage due to the underlying hematological disease, opportunistic infections in a setting of severe immunosuppression, and pharmacological toxicity of accompanying chemotherapy drugs are conditions that should be taken into consideration when evaluating the possible effects of CAR T-cell therapy. Fludarabine, a drug used for the conditioning with cyclophosphamide in all our cases, seems to promote a discernible form of neurotoxicity, with unspecific but distinctive gliosis and white matter involvement<sup>11</sup>. Basic neuropathologic assessment allows reliably detecting or discarding malignant cell infiltration in the central nervous system. It also enables to demonstrate the presence of inflammation with or without infectious agents in neurological tissue, although their absence does not completely rule out infection as in our fifth case.

Alterations of the BBB cannot be reliably studied in HE alone and specially without a prior technical background. Nevertheless, without clear evidence of brain weight gain, oedema, and white matter changes, nor minimal vascular damage and perivascular cellular reactions, BBB disruption may be at best limited in cases without neurological involvement in life. On the other hand, astrocyte injury can be highlighted with IHC showing GFAP aberrant beading and fragmentation, a phenomenon called clasmotodendrosis, that relates to blood barrier dysfunction<sup>8,15</sup>. We reexamined our cases with GFAP, and only saw scattered foci of clasmotodendrosis in 2 cases, one with hypoxic-ischemic changes in the context of nosocomial pneumonia and one with encephalomyelitis. Clasmotodendrosis has been related to acute metabolic disturbances in astrocytes (hypoxia, ischemia, hypoglycemia...) <sup>15</sup>, and as such may not be pathognomonic of CRS brain pathology or fludarabine neurotoxicity, for example, especially when is mild and focal and may have alternative causes. The relative lack of clasmotodendrosis as well as overall gliosis in most of our cases would sup-

port the notion that BBB dysfunction is not a systematic feature in CAR T-cell treated critical patients when they do not have specific and severe neurological symptomatology.

We present 6 patients who died after CAR T-cell therapy, 2 of whom displayed neurologic clinical manifestations with only one showing significant neuropathological findings. This case had an encephalomyelitis of immune-toxic versus infectious origin, being the findings in the rest of the patients unspecific and minimal, with mild chronic vascular disease and changes suggestive of terminal hypoxic-ischemic etiology. Interestingly, the encephalomyelitis changes could not be related to the presence of CAR T-cells in brain tissue, while we were able to demonstrate CAR T-cells in brain tissue of one patient without relevant histological changes nor neurological symptoms.

In conclusion, patients that die after CAR T-cell therapy show non-specific or minimal neuropathological changes, especially when they lack evident neurological symptoms and these do not contribute in patient death. CAR T-cell related direct toxicity may not be the only cause for neurological symptoms, and autopsy may detect other pathological processes, such as disease progression. CAR T-cell therapy is a new therapeutic approach that needs further research to elucidate its potential adverse effects and the underlying pathological mechanisms behind them.

## Conflicts of interest

The authors have no conflicts of interest that relate to the content of this article.

## Acknowledgments

We are thankful to the pathology technicians in the immunohistochemistry and molecular sections of the Pathology Department for the performed studies.

## Funding

The authors have not received specific funding for this study. CFL thanks the Spanish Institute of Health Carlos III (projects PI19/00669 and ICI19/00025; co-funded by the European Union).

## References

1. Kochenderfer, J. N. *et al*. Chemotherapy-refractory diffuse large B-cell lymphoma and indolent B-cell malignancies can be effectively treated with autologous T cells expressing an anti-CD19 chimeric antigen receptor. *J. Clin. Oncol.* **33**, 540–549 (2015). PMID: 25154820. <https://doi.org/10.1200/JCO.2014.56.2025>
2. Turtle, C. J. *et al*. CD19 CAR-T cells of defined CD4+:CD8+ composition in adult B cell ALL patients. *J. Clin. Invest.* **126**, 2123–2138 (2016). PMID: 27111235. PMCID: PMC4887159. <https://doi.org/10.1172/JCI85309>
3. Maude, S. L. *et al*. Chimeric Antigen Receptor T Cells for Sustained Remissions in Leukemia. *N. Engl. J. Med.* **371**, 1507–1517 (2014). PMID: 25317870. PMCID: PMC4267531. <https://doi.org/10.1056/NEJMoa1407222>
4. Turtle, C. J., Riddell, S. R. & Maloney, D. G. CD19-Targeted chimeric antigen receptor-modified T-cell immunotherapy for B-cell malignancies. *Clin. Pharmacol. Ther.* **100**, 252–258 (2016). PMID: 27170467. <https://doi.org/10.1002/cpt.392>
5. Turtle, C. J. *et al*. Immunotherapy of non-Hodgkin's lymphoma with a defined ratio of CD8+ and CD4+ CD19-specific chimeric antigen receptor-modified T cells. *Sci. Transl. Med.* **8**, 355ra116 (2016). PMID: 27605551. PMCID: PMC5045301. <https://doi.org/10.1126/scitranslmed.aaf8621>
6. Oliver-Caldes, A. *et al*. First report of CART treatment in AL amyloidosis and relapsed/refractory multiple myeloma. *J. Immunother. cancer* **9**, e003783 (2021). PMID: 34876408. PMCID: PMC8655576. <https://doi.org/10.1136/jitc-2021-003783>
7. Hunter, B. D. & Jacobson, C. A. CART-Cell Associated Neurotoxicity: Mechanisms, Clinicopathologic Correlates, and Future Directions. *J. Natl. Cancer Inst.* **111**, 646–654 (2019). PMID: 30753567. <https://doi.org/10.1093/nci/djz017>
8. Torre, M. *et al*. Neuropathology of a case with fatal CAR T-cell-associated cerebral edema. *J. Neuropathol. Exp. Neurol.* **77**, 877–882 (2018). PMID: 30060228. <https://doi.org/10.1093/jnen/nly064>
9. Gust, J. *et al*. Endothelial activation and blood–brain barrier disruption in neurotoxicity after adoptive immunotherapy with CD19 CAR-T cells. *Cancer Discov.* **7**, 1404–1419 (2017). PMID: PMC5718945. <https://doi.org/10.1158/2159-8290.CD-17-0698>
10. Schuster, S. J. *et al*. Chimeric Antigen Receptor T Cells in Refractory B-Cell Lymphomas. *N. Engl. J. Med.* **377**, 2545–2554 (2017). PMID: 29226764. PMCID: PMC5788566. <https://doi.org/10.1056/NEJMoa1708566>
11. Lowe, K. L. *et al*. Fludarabine and neurotoxicity in engineered T-cell therapy. *Gene Therapy.* **25**, 176–191 (2018). PMID: 29789639. <https://doi.org/10.1038/s41434-018-0019-6>
12. Ortíz-Maldonado, V. *et al*. CART19-BE-01: A Multicenter Trial of ARI-0001 Cell Therapy in Patients with CD19+ Relapsed/Refractory Malignancies. *Mol. Ther.* **29**, 636–644 (2021). PMID: 33010231. PMCID: PMC7854276. <https://doi.org/10.1016/j.ymthe.2020.09.027>
13. Castella, M. *et al*. Development of a Novel Anti-CD19 Chimeric Antigen Receptor: A Paradigm for an Affordable CAR T Cell Production at Academic Institutions. *Mol. Ther. - Methods Clin. Dev.* **12**, 134–144 (2019). PMID: 30623002. PMCID: PMC6319086. <https://doi.org/10.1016/j.omtm.2018.11.010>
14. Castella, M. *et al*. Point-Of-Care CAR T-Cell Production (ARI-0001) Using a Closed Semi-automatic Bioreactor: Experience From an Academic Phase I Clinical Trial. *Front. Immunol.* **11**, 482 (2020). PMID: 32528460. PMCID: PMC7259426. <https://doi.org/10.3389/fimmu.2020.00482>
15. Balaban, D., Miyawaki, E. K., Bhattacharyya, S. & Torre, M. The phenomenon of clasmotodendrosis. *Heliyon* **7**, e07605 (2021). PMID: 34368479. PMCID: PMC8326353. <https://doi.org/10.1016/j.heliyon.2021.e07605>